Biofilm 6 (2023) 100155

Contents lists available at ScienceDirect

Biofilm

journal homepage: www.sciencedirect.com/journal/biofilm

Glycosyl hydrolase from *Pseudomonas fluorescens* inhibits the biofilm formation of *Pseudomonads*

Di Wang [a,1], Syed Tatheer Alam Naqvi [a,1,2], Fanglin Lei [a,c,1], Zhenyu Zhang [a,b], Haiying Yu [a], Luyan Z. Ma [a,b,*]

[a] State Key Laboratory of Microbial Resources, Institute of Microbiology, Chinese Academy of Sciences, Beijing, 100101, PR China
[b] University of Chinese Academy of Sciences, Beijing, 100049, PR China
[c] Yunnan University, Kunming, 650500, PR China

ARTICLE INFO

Keywords:
Glycosyl hydrolase
Pseudomonas
Exopolysaccharides
Anti-biofilm

ABSTRACT

Biofilms are complex microbial communities embedded in extracellular matrix. Pathogens within the biofilm become more resistant to the antibiotics than planktonic counterparts. Novel strategies are required to encounter biofilms. Exopolysaccharides are one of the major components of biofilm matrix and play a vital role in biofilm architecture. In previous studies, a glycosyl hydrolase, $PslG_{PA}$, from *Pseudomonas aeruginosa* was found to be able to inhibit biofilm formation by disintegrating exopolysaccharide in biofilms. Here, we investigate the potential spectrum of PslG homologous protein with anti-biofilm activity. One glycosyl hydrolase from *Pseudomonas fluorescens*, $PslG_{PF}$, exhibits anti-biofilm activities and the key catalytic residues of $PslG_{PF}$ are conserved with those of $PslG_{PA}$. $PslG_{PF}$ at concentrations as low as 50 nM efficiently inhibits the biofilm formation of *P. aeruginosa* and disassemble its preformed biofilm. Furthermore, $PslG_{PF}$ exhibits anti-biofilm activity on a series of *Pseudomonads*, including *P. fluorescens, Pseudomonas stutzeri* and *Pseudomonas syringae* pv. *phaseolicola*. $PslG_{PF}$ stays active under various temperatures. Our findings suggest that *P. fluorescens* glycosyl hydrolase $PslG_{PF}$ has potential to be a broad spectrum inhibitor on biofilm formation of a wide range of *Pseudomonads*.

1. Introduction

Biofilms are complex microbial communities embedded in an extracellular matrix composed of proteins, extracellular DNA (eDNA), lipids, and exopolysaccharides [1,2]. Biofilms provide a number of advantages for bacteria survival and are extremely difficult to eradicate from living hosts or abiotic materials. The invulnerability of biofilm depends on a series of biofilm-specific characteristics including slow growth, physiologic heterogeneity of the inhabitants and sticky matrix [3]. In biofilms, bacteria can account for less than 10% of their dry mass, whereas matrix can account for over 90% [4,5]. The matrix is produced by the organisms themselves and composed of different types of biopolymers, known as extracellular polymeric substance (EPS) [6]. EPS helps the bacterial cells to live in close proximity and interact, which profoundly differs from their planktonic counterparts [7]. The EPS provides an extra covering around the cells providing a shield against various stresses. Bacteria within the biofilm are recalcitrant to antibiotics, environmental stresses and even escape host immune response. Therefore, bacterial biofilms cause serious problems in industry, agriculture as well as in clinical settings [8,9]. Exopolysaccharides, considered to be one of the important components of the biofilm matrix, act as a scaffold, to which carbohydrates, proteins, lipids and nucleic acid adhere, to form the biofilm matrix [10–12]. Exopolysaccharides play a vital role in cell-cell and cell-surface interaction and also provide bacteria a barrier against antibiotics and host defenses ([13], P. [14–16]).

Pseudomonas aeruginosa is an opportunistic pathogen that causes chronic infections in individuals with the genetic disease, cystic fibrosis (CF) [17,18]. *P. aeruginosa* can produce three known exoplysaccharides, namely alginate, Pel, and Psl. Each of them plays a unique role in biofilm development [19,20]. Psl consists of a repeating pentasaccharide of mannose, rhamnose, and glucose (3:1:1), and is considered to be the first line of defense towards various antibiotics during the early stages of biofilm development [21–23]. A polysaccharide locus termed

* Corresponding author. State Key Laboratory of Microbial Resources, Institute of Microbiology, Chinese Academy of Sciences, Beijing 100101, PR China.
E-mail address: luyanma27@im.ac.cn (L.Z. Ma).
[1] contributed equally.
[2] Present address: Department of Biotechnology, COMSATS University Islamabad, Abbottabad Campus, Abbottabad, Pakistan.

https://doi.org/10.1016/j.bioflm.2023.100155
Received 31 March 2023; Received in revised form 14 September 2023; Accepted 15 September 2023
Available online 16 September 2023
2590-2075/© 2023 The Authors. Published by Elsevier B.V. This is an open access article under the CC BY-NC-ND license (http://creativecommons.org/licenses/by-nc-nd/4.0/).

as *psl* is composed of 15 genes encoding the Psl biosynthetic machinery, which is essential for the biofilm formation of *P. aeruginosa* strains PAO1 and ZK2870 [24,25]. Psl is the critical component for *P. aeruginosa* to attach to different surfaces and required to maintain the biofilm structure at post attachment steps [25]. Enzymes capable to hydrolyze polysaccharides play a vital role in the inhibition of biofilms, as well as in the disruption of established biofilms and can be used as therapeutic agents [20]. Glycoside hydrolases (GHs) are enzymes that catalyze hydrolysis of the glycosidic linkages between two or more carbohydrates. A wide range of pathogens form biofilms with exopolysaccharides as their main component, where glycoside hydrolases break down the glycosidic linkage of exopolysaccharides and are able to disperse biofilms. In our previous study, we have reported a self-generated enzyme PslG from *P. aeruginosa* PAO1 that has the ability to hydrolyze exopolysaccharide Psl of *P. aeruginosa* and inhibit biofilm formation efficiently, as well as disrupt the preformed biofilms of various *Pseudomonas* species [26]. Interestingly, genes encoding glycoside hydrolases are always located in the gene operon involved in exopolysaccharide synthesis [27]. Baker et al. [28] expressed the glycoside hydrolases $PelA_h$ and $PslG_h$ from *pel* and *psl* operons and found that the enzymes can inhibit as well as disassemble the biofilms of *P. aeruginosa* [28]. Moreover, PslG also plays an important role in shaping bacteria cell fate and signaling [27]. Recently a bacterial amylase and fungal cellulase were used to disrupt the biofilms of *Staphylococcus aureus* and *P. aeruginosa*. Both of these enzymes could inhibit and disrupt the *S. aureus* and *P. aeruginosa* monoculture and co-culture biofilms [29].

In the present study, by postulating the hypothesis that enzymes from the glycoside hydrolases family can inhibit and disperse the bacterial biofilms, we investigated the potential spectrum of PslG homologous proteins with anti-biofilm activity in other *Pseudomonas* species, i. e. *Pseudomonas putida* KT2440*, Pseudomonas fluorescens* 17400*, Pseudomonas stutzeri* A1501*,* and *Pseudomonas syringae* pv. tomato DC3000. All of these four strains can form biofilms under certain conditions [30–33]. Similar as *P. aeruginosa, P. putida* and *P. fluorescens* are members of the *Pseudomonas* fluorescens group [34]. Strain *P. stutzeri* A1501 is an isolate from rhizosphere and capable of fixing nitrogen [35]. All the above three organisms are plant growth-promoting rhizobacteria (PGPRs) and also have a strong effect in bioremediation [36,37], while *P. syringae* pv. tomato DC3000 is a well-studied plant pathogen [38]. Homologs of $PslG_{PA}$ (glycoside hydrolase from *P. aeruginosa* PAO1) were selected from these four different species of *Pseudomonas*, and their anti-biofilm abilities were evaluated and compared with $PslG_{PA}$ in this work.

2. Materials and methods

2.1. Bacterial strains and growth conditions

Pseudomonas aeruginosa was grown in Luria Bertania (LB) at 37 °C or in Jensen's chemically defined medium [39]. Biofilm of *P. aeruginosa* was grown in Jensen's medium at 30 °C [26]. Biofilm of *Pseudomonas stutzeri* was grown in K-medium at 30 °C [40]. *Pseudomonas syringae* pv. *phaseolicola* biofilm was grown in MMX medium at 30 °C [41]. M63 supplemented with 0.2% glucose and 0.5% casamino acids or 0.4% sodium citrate as the growth substrate was used for the biofilm of *Pseudomonas fluorescens* [42,43]. Bacterial growth curve was carried out in 96-well plates (NEST Co., Wuxi, China). Bacteria culture was inoculated in 96-well plates with starting OD_{600} at 0.05 setting in a constant temperature microplate shaker (MIULAB Co., Hangzhou, China) at 37 °C for *P. aeruginosa*, and 30 °C for the other three Pseudomonads, with shaking at 700 rpm for 24 h. Bacterial growth was measured at 600 nm with gain 20 as scattered light using Synergy H4 hybrid reader (BioTek, USA).

2.2. Expression of glycosyl hydrolases from different Pseudomonas strains

Homologs of $PslG_{PAO1}$ (glycoside hydrolase from *P. aeruginosa* PAO1) were selected from *P. putida* KT2440*, P. fluorescens* 17400*, P. stutzeri* A1501*, P. syringae* pv. Tomato DC3000. In each case, signal peptides were predicted by using SignalP 5.0 server and the transmembrane region were predicted by using TMHMM-2.0 server (Services- DTU Health Tech). The gene responsible for the expression of glycoside hydrolases from each strain was amplified from the respective genomic DNA of the strain by using their respective primers shown in Table 1.

The gene (PST_2494) encoding glycoside hydrolase in *P. stutzeri* A1501 was amplified and cloned into an expression vector. For the expression of glycoside hydrolase, the sequence encoding glycoside hydrolase (residues 36–360) was amplified from the genomic DNA of the strain and cloned in PGLO1 at BamHI and XhoI sites. The first 35 amino acids were truncated as they were predicted to be signal peptides as well as transmembrane by the SignalP 5.0 server. The glycoside hydrolase was expressed in *E. coli* BL21(DE3) pLysS cells transformed with PGLO1:$PslG_{PSt}$. The overnight cultures of these cells were inoculated in LB with ampicillin (100 μg/ml) and incubated at 37 °C till OD_{600} reached 0.8. Then the culture was induced overnight with 0.05 mM isopropyl *β*-D-thiogalactopyranoside (IPTG) at 12 °C.

The glycoside hydrolase (PSPTO_3534) of *P. syringae* pv. tomato DC 3000 was amplified and cloned as described above. For its expression, the sequence encoding glycoside hydrolase, residues 30–437 was amplified and cloned in PGLO1. The resulted plasmids PGLO1:$PslG_{PSy}$ was transformed into *E. coli* BL21(DE3) pLysS cells and expressed in a similar way as described above.

Gene (PP_3139) encoding glycoside hydrolase in *P. putida* KT2440 was amplified from its genomic DNA. For the expression of glycoside hydrolase, the sequence encoding glycoside hydrolase (residues 1–400) was amplified and cloned in PGLO1. PGLO1:$PslG_{PP}$ was transformed in *E. coli* BL21(DE3) pLysS cells grown in LB-Ampicillin for about 2 h to get OD_{600} of 0.8 and then induced overnight with 0.05 mM isopropyl *β*-D-thiogalactopyranoside at 12 °C.

For the expression of glycoside hydrolase from *P. fluorescens* ATCC17400, the glycoside hydrolase encoding gene (BG51_RS0109500) was amplified from the *P. fluorescens* ATCC17400 and cloned in PGLO1. The resulted plasmids were transformed in *E. coli* BL21(DE3) pLysS and expressed in LB-Ampicillin. The culture was incubated at 37 °C for about 2 h to get an OD_{600} of 0.8 and then induced overnight with 0.05 mM isopropyl *β*-D-thiogalactopyranoside at 12 °C. Different truncated proteins were expressed along with the whole residues including signal peptides i.e. $PslG_{PF(1\text{-}446)}$, $PslG_{PF(9\text{-}446)}$, and $PslG_{PF(34\text{-}446)}$.

2.3. Purification of enzymes

The bacterial cells were harvested by centrifugation at 5000 rpm for 15 min at 4 °C. Harvested cells were re-suspended in phosphate buffer (pH 8). The bacterial cells were lysed by ultra-sonication and cell debris was removed by centrifugation (12000 rpm for 45 min) and supernatant was recovered. As his_6-tag was introduced during cloning, the supernatant was loaded on Ni-NTA column after equilibration with phosphate buffer (pH 8). The protein was eluted with a linear gradient of elution buffer (Phosphate buffer with 5% glycerol, pH 8) containing different molar concentrations of imidazole (20 mM–250 mM). Protein was monitored for its purity by SDS-PAGE (Fig. 1C). To remove the imidazole, buffer exchange was performed by using Superdex 200 increase column of GE Healthcare while using Tris-buffer (25 mM Tris with 100 mM NaCl, pH 7.5) as an exchange buffer to elute protein.

2.4. Protein secondary structure prediction and site-directed mutagenesis on predicted catalytic residues

Secondary structure of $PslG_{PF}$ was predicted with SWISS-MODEL (http://www.swissmodel.expasy.org). The three-dimensional (3D) protein modeling for $PslG_{PF}$ was obtained based on the reference structure of $PslG_{PA}$ (PDB No. 5bx9) using Swiss-PdbViewer 4.1 molecular visualization software. The catalytic residues of the enzyme were predicted by

Table 1
Primers used for the amplification of glycoside hydrolase genes from different bacterial strains.

S.No	Bacterial strain/gene ID	Sequence of primers
1	*Pseudomonas syringae* pv. Tomato DC3000, PSPTO_3534	PSPF: TGTTCCAGGGGCCCGGATCCATGCTCAAAGGCCCGCGCGAAGTGGTCTG PSPR: CTTTACCAGACTCGAGTTAGGGCTTCCATTCCAGG
2	*Pseudomonas stutzeri* A1501, PST_2494	PSTF: TGTTCCAGGGGCCCGGATCCATGCAATGACGAAGGAGGCCTGG PSTR: CTTTACCAGACTCGAGTCAATCAGCAATTTGCGCAGGTGTAGG
3	*Pseudomonas putida* KT 2440, PP_3139	PPF: TGTTCCAGGGGCCCGGATCCATGCGCATTGCTTAC PPR: CTTTACCAGACTCGAGTCATGCGTATGC
4	*Pseudomonas fluorescens* ATCC 17400 BG51_RS0109500	$PFF_{(1-446)}$: TGTTCCAGGGGCCCGGATCCATGAACACGTC $PFF_{(9-446)}$: TGTTCCAGGGGCCCGGATCCATGTGGCGCTAC $PFF_{(34-446)}$: TGTTCCAGGGGCCC**GGATCCAT**GAGCCGGTCAACC PFR: CTTTACCAGACTCGAGCTACCACACC
5	*Pseudomonas fluorescens* ATCC 17400 BG51_RS0109500 (for site-directed mutagenesis at E168 and E281)	E168F: CAGGTGTGGAACAAACAGAACCTGCCGAAC (complement at 5′end) E168R: GGTTCTGTTTGTTCCACACCTGCCAGGCGTTGATATTC (complement at 5′end) E281F: ATGTCTGGGCCACCAAGTGGGGCTGGTCC (complement at 5′end) E281R: CACTTGGTGGCCCAGACATCCTTGACCCC (complement at 5′end)

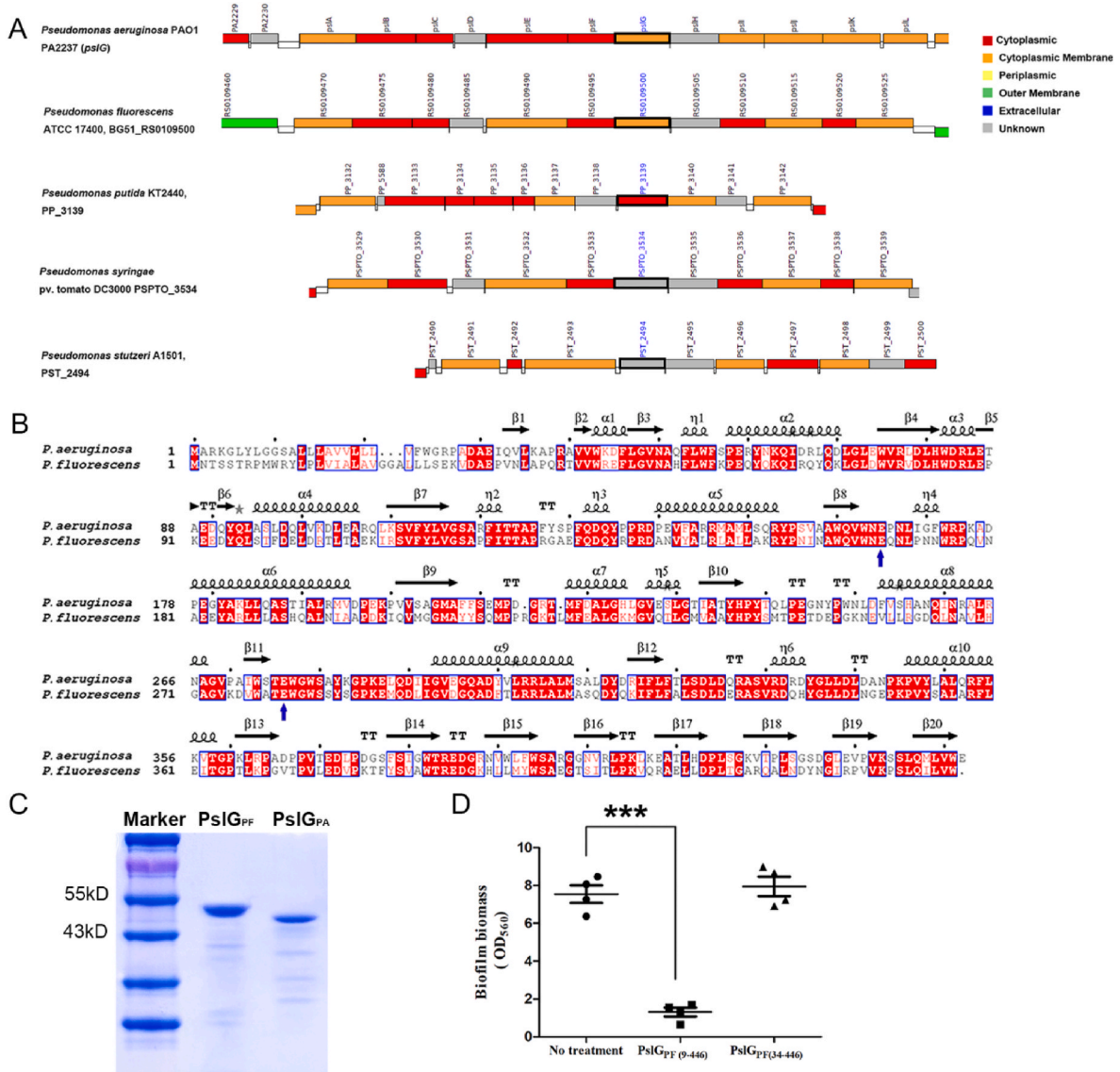

Fig. 1. Biofilm inhibition ability of PslG from *Pseudomonas fluorescens* ATCC 17400 ($PslG_{PF}$) (A) Homologs of $pslG_{PA}$ identified in exopolysaccharides gene clusters from other *Pseudomonas* species. The black boxed genes are *pslG* homologous genes. (B) Protein sequence alignment between $PslG_{PF}$ and $PslG_{PA}$. Arrows indicate the two predicted catalytic residues according to previously reported $PslG_{PA}$ catalytic residues [26]. (C) SDS-PAGE gel of purified $PslG_{PF9-446}$. $PslG_{PA}$ protein is loaded as a control. (D) The ability of $PslG_{PF}$ truncated at different sites at N-terminal to inhibit biofilm formation of *P. aeruginosa*. Experiments were carried out in four replicates. Significance was determined by using a one-way ANOVA, and error bars indicate standard deviations (***$p < 0.001$).

using the COACH server [44]. Predicted sites E168 and E281 were mutated by site-directed mutagenesis. Glutamic acid at position E168 and E281 was replaced with lysine, respectively. In each case the plasmid PGLO1:PslG$_{PF(9-446)}$ were used as template for DNA amplification with respective primers (Table 1) [45]. The PCR reaction mixture for site-directed mutagenesis contained high-fidelity DNA polymerase, 5× Phusion buffer (with dNTPs), reverse and forward primers, and distilled water. After denaturation at 98 °C for 30 s, 30-cycle of amplification (98 °C for 30 s, 69 °C for 30 s and 72 °C for 2 min) were performed followed by a final extension of 72 °C for 5 min. The resulted plasmids were cloned in DH5α and sequenced. The plasmids carrying the required mutation were transformed into *E. coli* BL21(DE3) pLysS cells and protein was purified as described above by using Ni-NTA column.

2.5. Circular dichroism spectroscopy of purified PslG$_{PF}$ protein

Ultraviolet circular dichroism (CD) spectroscopy was applied to investigate whether the site-mutated variants of PslG$_{PF}$ still kept the secondary structures of native form of PslG$_{PF}$. 200 μl of 0.2 mg/ml of each purified protein was loaded into the ultraviolet circular dichroism spectrometer (Chirascan, AppliedPhotophysics, UK). Circular Dichroism data were collected at every 0.5 nm wavelength. Experiments were carried out in triplicate.

2.6. Biofilm inhibition and disassembly assay

Crystal violet (CV) biomass assay was performed for the estimation of enzyme inhibition as well as disassembly of biofilms. For biofilm inhibition assay, overnight culture was inoculated at 1/100 for *P. aeruginosa*, or 1:15 for *P. stutzeri* and *P. syringae* pv. *phaseolicola* in 96 microtiter dish into appropriate medium, respectively. Planktonic cells were washed off after 24 h for *P. aeruginosa* and *P. stutzeri*, or 72 h for *P. syringae* pv. *phaseolicola* of static incubation at 30 °C, and the attached cells in 96 well were stained with 0.1% crystal violet for 15 min [46]. The microtiter dish was washed thoroughly. The crystal violet bound to biofilms was dissolved in 30% acetic acid and measured the absorbance at 560 nm. For biofilm disassembly assay, preformed biofilm was treated with the 50 nM of PslG$_{PF}$ and incubated at 30 °C. The CV biomass assay was performed after various intervals of time. Experiments were carried out in triplicate. Significance was determined by using a one-way ANOVA analysis.

2.7. Confocal laser scanning microscopy (CLSM)

The air–liquid interface biofilms (pellicles) of *P. stutzeri* A1501 were grown in glass chambers (Chambered #1.5 German Coverglass System, Nunc, New York, NY, USA) with or without 50 nM of PslG$_{PF}$ treatment at 30 °C for 24 h. For CLSM observation, buffer was gently removed, and the pellicles were washed with saline solution twice. The biofilms were stained by live-dead staining kit with SYTO9 and propidium iodide (Costerton, Lewandowski et al.) following the instruction of the manufacturer (Molecular Probes, Invitrogen), and fluorescent images were acquired by Leica SP8 CLSM (Leica Microsystems, Germany). CLSM-captured images were subjected to quantitative image analysis using COMSTAT software as previously described [47].

2.8. Degradation of Psl by PslG$_{PF}$ in vitro

Psl polysaccharide extract was prepared as previously described with modifications [21]. Crude Psl polysaccharide was subsequently treated with 0.1 mg/ml DNaseI (Sigma) and proteinase K to remove DNA and proteins from exopolysaccharides, as previously described [26]. To test the ability of PslG$_{PF}$ to degrade Psl polysaccharide, 4 mg/ml of Psl was incubated with or without 50 nM of PslG$_{PF}$ for 2 h at 30 °C. PslG$_{PA}$ was applied as a positive control. Inactivated PslG$_{PF}$ was prepared with heat treated at 100 °C for 30 min. Treated or untreated Psl samples were examined by immunoblotting against anti-Psl serum, as previously described [21]. ImageJ was used to quantify the immunoblotting data. Quantitation of Psl was carried out by converting the grayscale value to the Psl concentration according to the corresponding standard Psl polysaccharide curves.

2.9. Data analysis

Experiments were carried out in three to five biological replicates. Significance was determined by using a one-way ANOVA. Results with p-value smaller than 0.05 are considered as statistically significant.

3. Results

3.1. Purification of homologous protein of Pseudomonas aeruginosa glycosyl hydrolases PslG from various bacteria

We investigated the homologous proteins of *Pseudomonas aeruginosa* glycoside hydrolases PslG from other four *Pseudomonas* species, i.e *Pseudomonas putida* KT2440, *Pseudomonas fluorescens* 17400, *Pseudomonas stutzeri* A1501, and *Pseudomonas syringae* pv. tomato DC3000. These four *Pseudomonas* strains all carried glycoside hydrolase gene located in the gene clusters involved in the exopolysaccharide synthesis, which is similar as *psl* operon in *P. aeruginosa* PAO1 (Fig. 1A). These *pslG* homologous genes were amplified and proteins were expressed using *E. coli* BL21 strain. One active glycoside hydrolase was obtained from *pslG* of *P. fluorescens* ATCC 17400. Protein sequence alignment showed that PslG$_{PF}$ shared 56.25% identity with previously reported glycoside hydrolase PslG of *P. aeruginosa* PAO1 (termed as PslG$_{PA}$, to distinguish with PslG$_{PF}$) (Fig. 1B). Signal peptide and transmembrane region analysis indicated that residues 1st −33rd is the signal peptide of PslG$_{PF}$ and residues 1st -8th stay inside of the membrane. Thus, PslG$_{PF}$ was expressed from three different starting sites at N terminal, which are PslG$_{PF(1-446)}$, PslG$_{PF(9-446)}$, and PslG$_{PF(34-446)}$. PslG$_{PF(9-446)}$ and PslG$_{PF(34-446)}$ were obtained in soluble form (Fig. 1) except of PslG$_{PF(1-446)}$. As PslG$_{PA}$ has been reported to efficiently inhibit the biofilm formation of *P. aeruginosa* PAO1, we tested the anti-biofilm activity of PslG$_{PF(9-446)}$ and PslG$_{PF(34-446)}$ by evaluating their capacity of inhibiting the biofilm formation of *P. aeruginosa*. PslG$_{PF(34-446)}$ showed no activity against biofilm formation (Fig. 1D). However, PslG$_{PF(9-446)}$ was able to inhibit the biofilm formation of *P. aeruginosa* (Fig. 1D), and its name was simplified as PslG$_{PF}$ in the following work.

3.2. Characterization of PslG$_{PF}$

In order to confirm the active site of the enzyme PslG$_{PF}$, we compared the amino acid sequences between PslG$_{PF}$ and PslG$_{PA}$ (Fig. 1B), then we predicted the three-dimensional structures of PslG$_{PF}$ by 3-D protein modeling based on the crystal structure of PslG$_{PA}$ (Fig. 2A). The catalytic residues of PslG$_{PA}$ have been confirmed previously [26]. Protein sequence alignment between these two glycoside hydrolases showed that residue Glu168 (E168) and Glu281 (E281) of PslG$_{PF}$ matched well with the catalytic residues in PslG$_{PA}$, Glu165 and Glu276, respectively (Fig. 1B). We then mutated these two amino acids using site-directed mutagenesis individually. In each case, glutamic acid was replaced with lysine and the mutated proteins were termed as PslG$_{PF}^{E168K}$ and PslG$_{PF}^{E281K}$, respectively. These mutated proteins were then applied to circular dichroism spectroscopy to determine whether mutated proteins were misfolded after site-mutation at E168 or E281. Circular dichroism of mutated proteins, PslG$_{PF}^{E168K}$ and PslG$_{PF}^{E281K}$, were the same as that of the native PslG$_{PF}$ protein (Fig. 2B), indicating that the secondary structure did not change in the mutated proteins. Then, we tested the ability of PslG$_{PF}^{E168K}$ and PslG$_{PF}^{E281K}$ to inhibit the biofilm formation of *P. aeruginosa*. It showed that PslG$_{PF}^{E168K}$ and PslG$_{PF}^{E281K}$ lost their ability to prevent the biofilm formation of *P. aeruginosa* (Fig. 2C), suggesting that

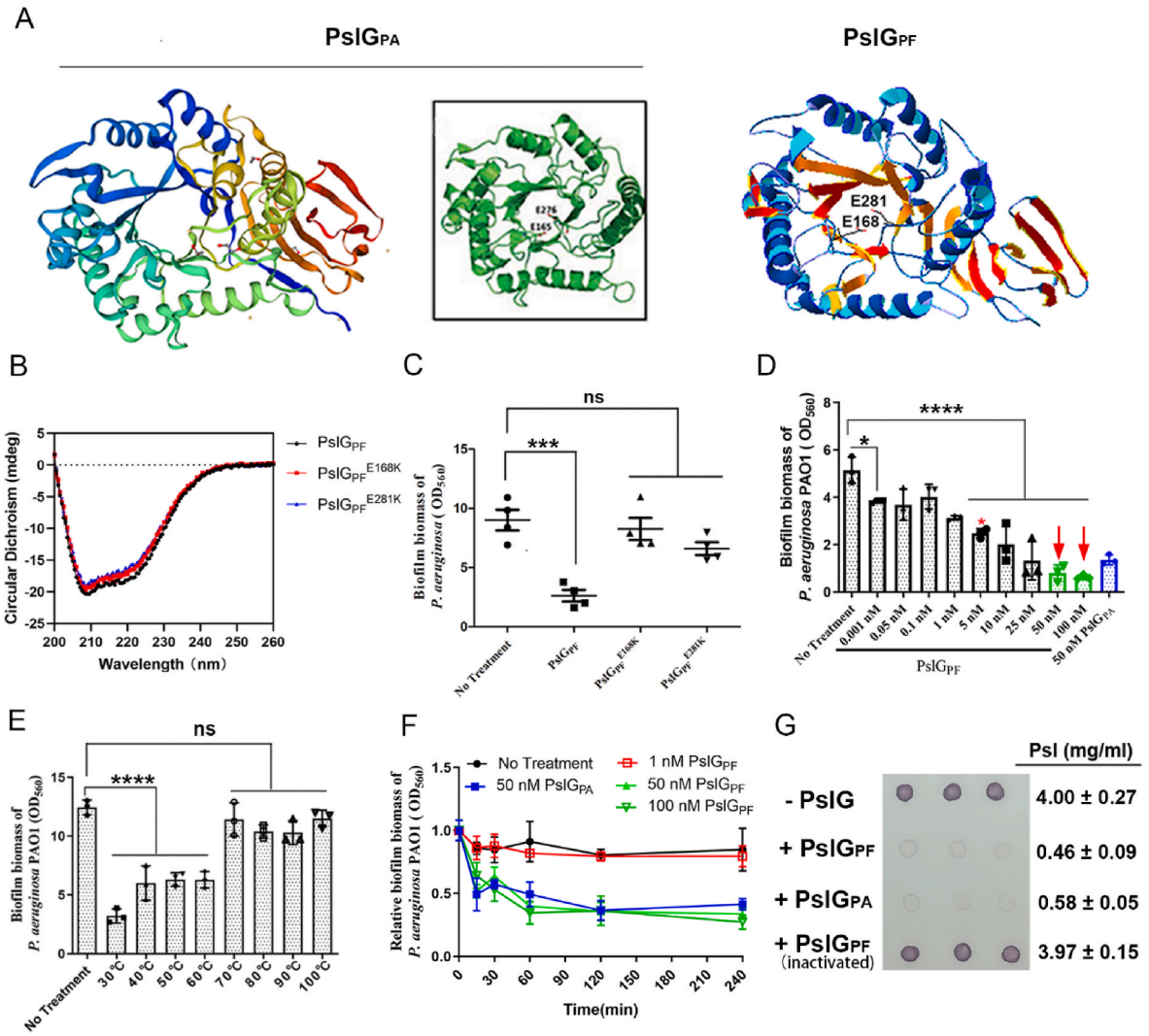

Fig. 2. Characterization of $PslG_{PF}$. (A) The three-dimensional (3D) protein modeling for $PslG_{PF}$, using $PslG_{PA}$ (PDB No. 5bx) as a reference [26]. The catalytic domain of $PslG_{PA}$ is presented in box. (B) Circular dichroism of purified $PslG_{PF}$ protein and its mutants, $PslG_{PF}^{E168K}$ and $PslG_{PF}^{E281K}$. (C) Anti-biofilm activity of $PslG_{PF}$ variants with catalytic residues mutated. (D) Minimum inhibitory concentration and (E) thermal stability of $PslG_{PF}$ determined by evaluating inhibition effect of $PslG_{PF}$ on *P. aeruginosa* biofilm formation. (F) Disassembly ability of $PslG_{PF}$ on preformed biofilms of *P. aeruginosa* PAO1. (G) Psl immunoblotting assay to determine the hydrolysis activity of $PslG_{PF}$ on purified Psl exopolysaccharide. Experiments were carried out in 3–4 replicates. Significance was determined by using a one-way ANOVA, and error bars indicate standard deviations (*$p < 0.05$; ***$p < 0.001$; ****$p < 0.0001$; ns, non-significant). Red star in panel D indicates the concentration of $PslG_{PF}$ that reduced half of the biofilm biomass, while arrows indicate the most effective concentrations of $PslG_{PF}$ to inhibit biofilm formation. (For interpretation of the references to colour in this figure legend, the reader is referred to the Web version of this article.)

both E168 and E281 are the key catalytic residues of $PslG_{PF}$.

To determine the ability of $PslG_{PF}$ to inhibit biofilm formation, various concentrations (0.001 nM–100 nM) of purified $PslG_{PF}$ was added to the biofilm-growing culture of *P. aeruginosa* PAO1 at inoculation. PslG from *P. aeruginosa* PAO1 strain ($PslG_{PA}$), which has been proved able to inhibit *P. aeruginosa* biofilms efficiently, was applied for comparison [26]. Biofilms were grown for 24 h. It was found that 0.001 nM of $PslG_{PF}$ was the minimum concentration that exhibited inhibitory ability, while higher concentration of $PslG_{PF}$ significantly enhanced the inhibition efficiency (Fig. 2D). 5 nM of $PslG_{PF}$ reduced half of the biofilm biomass of PAO1, while 50 nM and 100 nM were the most effective concentrations. Since 50 nM and 100 nM of $PslG_{PF}$ had the same efficacy, we then conducted the following experiments with 50 nM of $PslG_{PF}$ (Fig. 2D).

$PslG_{PF}$ was also tested for its thermal stability. $PslG_{PF}$ was incubated at various temperatures for 15 min and its activity was evaluated in biofilm inhibition assay against *P. aeruginosa* PAO1 biofilms, as described above. It was found that the $PslG_{PF}$ was robust in nature and it stayed stable and worked efficiently to inhibit PAO1 biofilm formation even after being heated at 60 °C for 15 min (Fig. 2E). The optimum temperature of $PslG_{PF}$ protein is 30 °C (Fig. 2E), which is consistent with the temperature of the habitats of *P. fluorescens*, 25–30 °C.

3.3. Extrogenously applied *P. fluorescens* $PslG_{PF}$ disassembles *P. aeruginosa* preformed biofilm

After confirming the role of $PslG_{PF}$ in inhibiting *P. aeruginosa* PAO1 biofilm formation, we asked whether *P. fluorescens* $PslG_{PF}$ could disassemble *P. aeruginosa* PAO1 exsiting biofilms. The biofilm disassembly assay was performed on mature biofilms formed by *P. aeruginosa* PAO1 after 24 h of incubation in Jensen's media. The biofilms were treated with purified $PslG_{PF}$ while incubating at 30 °C for 8 h. Our results showed that 50 nM of $PslG_{PF}$ exhibited strong disassembly activity on *P. aeruginosa* PAO1 preformed biofilms, while 100 nM of $PslG_{PF}$ showed a similar level of disassembly activity as that of 50 nM of $PslG_{PF}$ (Fig. 2F). A lower concentration of $PslG_{PF}$, which did not inhibit biofilm formation as much as did 50 nM, was also included in this experiment as

a control. 1 nM of $PslG_{PF}$ could not disassemble the preformed biofilm, indicating that it was indeed the enough amount of $PslG_{PF}$, rather than anything else that may exist in the protein buffer, disassembling the biofilm (Fig. 2F). Different time intervals of test showed that it took about 60 min for $PslG_{PF}$ to disassemble *P. aeruginosa* PAO1 biofilm by 60% (Fig. 2F), suggesting that exogenous addition of $PslG_{PF}$ with concentration as low as 50 nM was enough to efficiently disassemble the preformed biofilms of *P. aeruginosa*.

We speculated that the ability of $PslG_{PF}$ to inhibit biofilm formation and disassembling biofilms of *P. aeruginosa* was due to its hydrolase activity on exopolysaccharide. To confirm this speculation, we determined the ability of $PslG_{PF}$ to degrade *P. aeruginosa* Psl exopolysaccharide by immunoblotting using anti-Psl serum. Psl exopolysaccharide was incubated at 30 °C with or without 50 nM of $PslG_{PF}$ for 2 h. Immunoblotting showed that only less than 10% of the Psl was detected by Psl antibody after 2 h of $PslG_{PF}$ treatment (Fig. 2G), suggesting that $PslG_{PF}$ was able to degrade Psl exopolysaccharide. The hydrolase activity of $PslG_{PF}$ on *P. aeruginosa* Psl was comparable to that of $PslG_{PA}$ from *P. aeruginosa* (Fig. 2G) and the inactived $PslG_{PF}$ was used as a negative control [26].

3.4. $PslG_{PF}$ efficiently inhibited biofilm formation of different Pseudomonas strains

To investigate the application range of $PslG_{PF}$ at preventing biofilm formation, we evaluated the ability of $PslG_{PF}$ to prevent the biofilm formation of several other *Pseudomonas* species, including *P. aeruginosa*, *P. fluorescens, P. stutzeri* and plant pathogen *P. syringae* pv. *phaseolicola*. $PslG_{PA}$ from *P. aeruginosa* was applied for comparison [26]. 50 nM of $PslG_{PF}$ could significantly reduced the biofilm formation of *P. fluorescens* by 80%, while 50 nM of $PslG_{PA}$ only reduced *P. fluorescens* biofilm formation by 25% (Fig. 3B). Remarkably, $PslG_{PF}$ also exhibited strong ability to inhibit biofilms of *P. stutzeri* and *P. syringae* pv. *phaseolicola*. With $PslG_{PF}$ treatment, the biofilm biomass of *P. syringae* pv. *phaseolicola* was reduced by half (Fig. 3C), while *P. stutzeri* A1501 biofilm was reduced by 60% (Fig. 3D). Although $PslG_{PF}$ was not as efficient as $PslG_{PA}$ at inhibiting biofilm formation of *P. aeruginosa* (Fig. 3A), it exhibited higher activity at inhibiting biofilm formation of the other three *Pseudomonads* compared to $PslG_{PA}$ (Fig. 3B–D). Growth of these *Pseudomonas* strains were not affected by $PslG_{PF}$ (Fig. 3E–H), indicating that the inhibition effect of $PslG_{PF}$ on biofilms was not due to killing bacteria. However, $PslG_{PF}$ was unable to disassemble the preformed biofilm of *P. fluorescens*, *P. stutzeri* A1501 or *P. syringae* pv. *phaseolicola* (data not shown), even though it inhibited their biofilm formation efficiently (Fig. 3).

P. stutzeri A1501 could form biofilm at air-liquid interface which was termed as pellicle [32]. We applied $PslG_{PF}$ while growing *P. stutzeri* A1501 pellicles in 24-well plate. It showed that $PslG_{PF}$ significantly affected the pellicle formation of *P. stutzeri* A1501 within 1 day (Fig. 4). *P. stutzeri* A1501 pellicles with or without $PslG_{PF}$ treatment were observed under Confocal Laser Scanning Microscope (CLSM). $PslG_{PF}$ treatment remarkably reduced the biofilm biomass of *P. stutzeri* A1501 pellicles under both nitrogen rich (N+) or nitrogen deplete (N-) conditions (Fig. 4). With $PslG_{PF}$ treatment in N- medium, *P. stutzeri* A150 pellicles showed more holes compared to untreated pellicles. In N+ medium, *P. stutzeri* A1501 could hardly form pellicles with $PslG_{PF}$ treatment (Fig. 4). However, $PslG_{PF}$ treatment did not cause any increase in the Dead/Live ratio in *P. stutzeri* A1501 pellicles (Fig. 4), suggesting that the reduced biofilm biomass in $PslG_{PF}$ treatment was more likely through disassembly of biofilm matrix, rather than killing bacteria.

4. Discussion

Bacterial biofilms provide protective coverings to the microbes that are extremely recalcitrant to antibiotics and host defenses [6,17,48]. Exopolysaccharides are the main components of biofilm matrix, which play a vital role in antibiotic susceptibility, and contribute to the biofilm-associated chronic diseases [15,22,23,49]. Therefore, the strategies that aimed at degradation of exopolysaccharides and dispersing the bacteria back into their planktonic state, would be helpful for curing and healing the diseases [50]. Flemming et al. (2017) tested bacterial α-amylase (from *Bacillus subtilis*) and fungal cellulose (from *Aspergillus niger*) against the biofilm of *P. aeruginosa* and *Staphylococcus aureus* and found to be efficient to inhibit biofilms of both pathogens. Dispersin B (DspB) was also reported to play a vital role in disruption of extracellular matrix and biofilm biomass [51–53]. In the present study, a glycoside hydrolase $PslG_{PF}$ was found to be effective to prevent the biofilm formation of *P. fluorescence* itself and several other *Pseudomonads* (Figs. 1 and 4).

In biofilms, EPS have various glycosidic linkages that can be hydrolyzed by various enzymes from the glycoside hydrolases family. Each enzyme can be characterized by its ability to catalyze specific linkage. For example, α-amylase hydrolyzes α-1, 4 bond, while cellulase cleaves β-1, 4 bond and β-1, 3 galactosidase hydrolyzes β-1, 3 bond [54,55]. Therefore, enzymes belong to the glycoside hydrolase family are the key determinants to cleave glycosidic linkages in the EPS and play a major

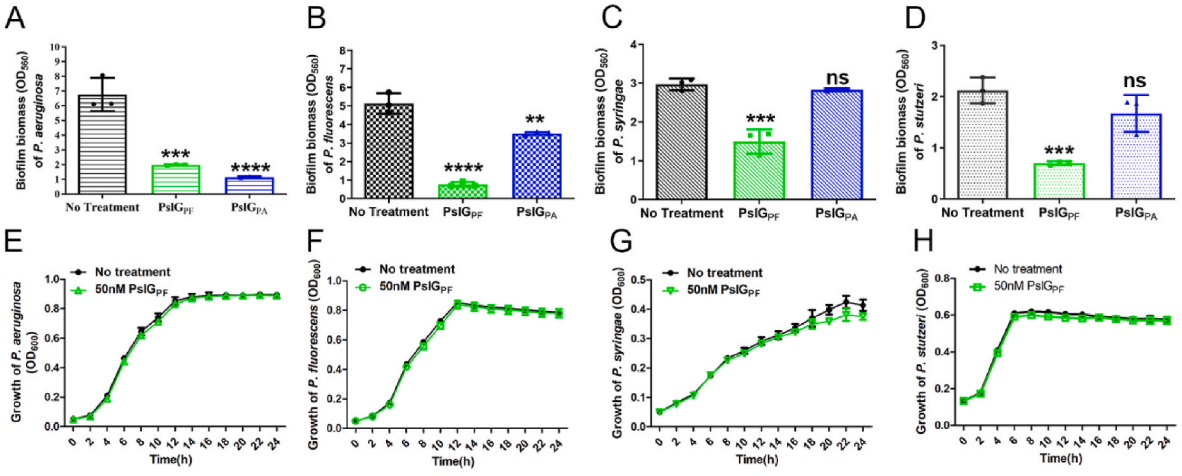

Fig. 3. The inhibition ability of $PslG_{PF}$ on the biofilm formation of (A) *P. aeruginosa*; (B) *P. fluorescens*; (C) *Pseudomonas syringae pv. Phaseolicola*; (D) *Pseudomonas stutzeri* A1501. $PslG_{PA}$ from *P. aeruginosa* PAO1was applied for comparison. The effect of $PslG_{PF}$ on the growth of (E) *P. aeruginosa*, (F) *P. fluorescens*; (G) *P. syringae pv. phaseolicola*; and (H) *P. stutzeri*, is presented. Experiments were carried out in triplicate. Significance was determined by using a one-way ANOVA, and error bars indicate standard deviations (**p < 0.01; ***p < 0.001; ****p < 0.0001; ns, non-significant).

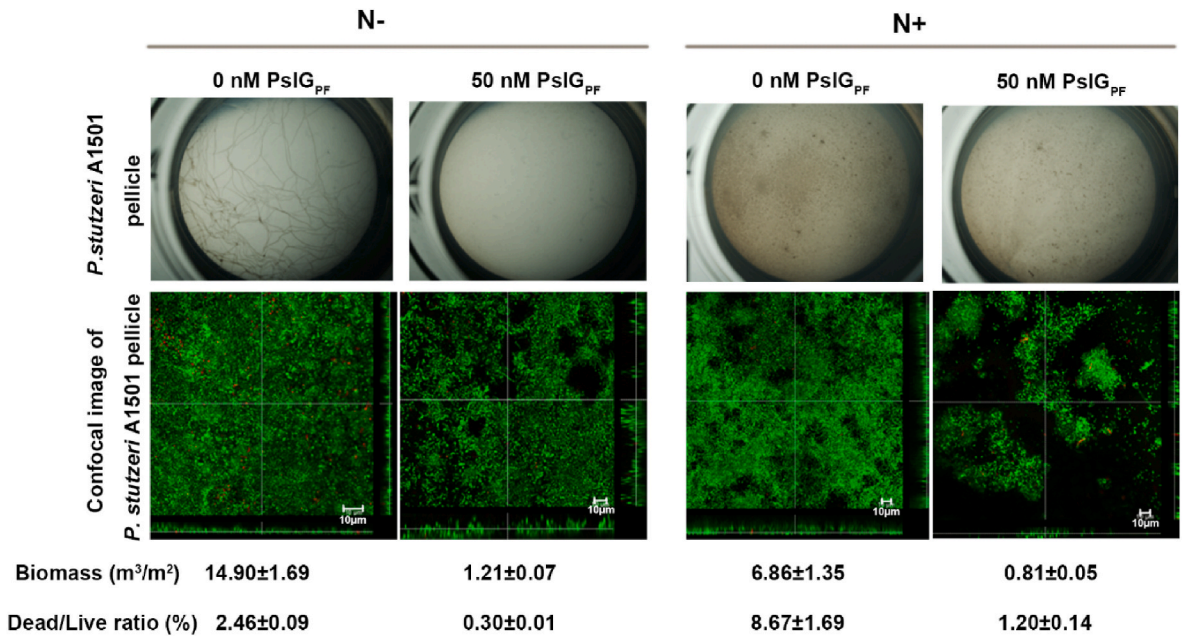

Fig. 4. The pellicle of *P. stutzeri* A1501 grown under either nitrogen deplete (N-) or nitrogen rich (N+) conditions, with or without PslG$_{PF}$ treatment. Pellicles were stained with live/dead staining kit and observed under confocal laser scanning microscope, with green fluorescence of syto9 indicated live cells and red fluorescence of PI indicated dead cells. Experiments were carried out in triplicate. Five images from each sample were used for the quantification. Scale bars, 10 μm. (For interpretation of the references to colour in this figure legend, the reader is referred to the Web version of this article.)

role in disruption of biofilm matrix. This disruption leads to the disassembly of bacterial community and also allows antibiotics to diffuse into the biofilm [26,28,56]. In the present work, glycoside hydrolase PslG$_{PF}$ from *P. fluorescens* was over-expressed and tested for its anti-biofilm activity. It is able to prevent the biofilm formation of human pathogen *P. aeruginosa*. Furthermore, PslG$_{PF}$ exhibited higher efficacy to prevent biofilm formation of a series of environmental *Pseudomonads*, including *P. fluorescens, P. stutzeri* and *P. syringae,* than did the PslG$_{PA}$ from *P. aeruginosa* PAO1. All the strains we studied in this work have a similar gene cluster as Psl gene cluster in *P. aeruginosa*. However, the structure of exopolysaccharides encoded by homologue of Psl genes in other pseudomonads have not been characterized. It is not clear whether the exopolysaccharides are different among these strains. We have tried to use Psl-antibody and lectin that can detect the Psl exopolysaccharide of *P. aeruginosa* to examine the exopolysaccharide in the biofilms formed by either *P. stutzeri* or *P. fluorescens*. The result showed a very weak signal, suggesting that the structure of exopolysaccharides produced by *P. stutzeri* or *P. fluorescens* are not the same as Psl of *P. aeruginosa*. However, based on our data in this manuscript, these exopolysaccharides might share similar glycosidic bonds which could be recognized by PslG$_{PA}$ or PslG$_{PF}$. Interestingly, PslG$_{PF}$ disassembled the preformed biofilm of pathogen *P. aeruginosa* within 60 min at 50 nM of concentration, but could not disassemble the biofilms of other three environmental isolated *Pseudomonads*. This may due to the differences of exopolysaccharides composition among *Pseudomonas* species.

It is worth to mention that although both PslG$_{PF}$ and PslG$_{PA}$ are glycoside hydrolases and share over 50% identity in amino acid sequences, they are truncated from different starting sites to obtain active proteins. In a previous study, it had to eliminate the signal peptide (1–30 aa) of PslG$_{PA}$ to keep it soluble and stay active [26], while in the present work, only the first 8 residues were truncated off to get an active form of PslG$_{PF}$ protein. We attempted to express PslG$_{PF}$ from the 34th amino acid to eliminate its signal peptide, but PslG$_{PF(34\text{-}446)}$ was not active (Fig. 1). Based on the result that PslG$_{PF(9\text{-}446)}$ is much more active than PslG$_{PF34\text{-}446}$, it cannot exclude the possibility that PslG$_{PA(9\text{-}442)}$ might exhibit even higher anti-biofilm ability than that of PslG$_{PA31\text{-}442}$. The catalytic residues of PslG$_{PF}$ have been clarified in our present study, which are consistent with those of PslG$_{PA}$. PslG$_{PF}$ exhibits excellent thermal stability even at 60 °C, which enables it to fit in a wide range of environmental conditions. PslG$_{PA}$ has been reported to have the maximal activity at 45 °C [26], while the optimal temperature for PslG$_{PF}$ is 30 °C. This may be due to the differences of the original habitats between these two organisms, with *P. aeruginosa* isolated from patients and *P. flourescens* commonly isolated from soil, water or rhizosphere. Thus, these two glycoside hydrolases may have application potential in different fields in future.

We observed many holes in PslG$_{PF}$-treated pellicles of *P. stutzeri* A1501, which is presumably due to the PslG$_{PF}$ hydrolyzation on the exopolysaccharides matrix to reduce the stability of EPS matrix. Moreover, the Dead/Live cells ratio of PslG$_{PF}$-treated pellicles was not increased compared to the untreated pellicles, suggesting that PslG$_{PF}$ does not kill bacteria cells. Growth curves of all the tested Pseudomonads also indicated that the presence of PslG$_{PF}$ did not affect bacterial growth. This is a great characteristic because it will not bring any stress to pathogens as antibiotics did, thus the pathogens will not easily generate resistance to this glycoside hydrolase, PslG$_{PF}$. Taken together, PslG$_{PF}$ has a great potential in anti-biofilm applications in many fields, including environmental remediation, agricultural biocontrol and food processing technologies.

Funding

This work is supported by the National Key R&D Program of China (2021YFA0909500, 2019YFC1804104, 2021YFC2301004, and 2019YFA0905501) and the National Natural Science Foundation of China (32070033, 91951204).

CRediT authorship contribution statement

Di Wang: Investigation, Validation, Writing – original draft, Writing – review & editing, Formal analysis, Supervision, Funding acquisition, contributed equally. **Syed Tatheer Alam Naqvi:** Investigation, Data curation, Writing – original draft, contributed equally. **Fanglin Lei:** Investigation, Data curation, Validation, contributed equally. **Zhenyu**

Zhang: Investigation. **Haiying Yu:** Data curation, Funding acquisition. **Luyan Z. Ma:** Conceptualization, Project administration, Supervision, Funding acquisition.

Declaration of competing interest

The authors declare that they have no known competing financial interests or personal relationships that could have appeared to influence the work reported in this paper.

Data availability

No data was used for the research described in the article.

References

[1] Irie Y, Starkey M, Edwards AN, Wozniak DJ, Romeo T, Parsek MR. Pseudomonas aeruginosa biofilm matrix polysaccharide Psl is regulated transcriptionally by RpoS and post-transcriptionally by RsmA. Mol Microbiol 2010;78(1):158–72.

[2] Jennings LK, Storek KM, Ledvina HE, Coulon C, Marmont LS, Sadovskaya I, Secor PR, Tseng BS, Scian M, Filloux A, Wozniak DJ, Howell PL, Parsek MR. Pel is a cationic exopolysaccharide that cross-links extracellular DNA in the Pseudomonas aeruginosa biofilm matrix. Proc Natl Acad Sci USA 2015;112(36):11353–8.

[3] Jefferson KK. What drives bacteria to produce a biofilm? FEMS Microbiol Lett 2004;236(2):163–73.

[4] Blackledge MS, Worthington RJ, Melander C. Biologically inspired strategies for combating bacterial biofilms. Curr Opin Pharmacol 2013;13(5):699–706.

[5] Su Y, Yrastorza JT, Matis M, Cusick J, Zhao S, Wang G, Xie J. Biofilms: formation, research models, potential targets, and methods for prevention and treatment. Adv Sci 2022;9(29):e2203291.

[6] Flemming HC, Wingender J. The biofilm matrix. Nat Rev Microbiol 2010;8(9):623–33.

[7] Hu W, Li L, Sharma S, Wang J, McHardy I, Lux R, Yang Z, He X, Gimzewski JK, Li Y, Shi W. DNA builds and strengthens the extracellular matrix in myxococcus xanthus biofilms by interacting with exopolysaccharides. PLoS One 2012;7(12):e51905.

[8] Høiby N, Bjarnsholt T, Givskov M, Molin S, Ciofu O. Antibiotic resistance of bacterial biofilms. Int J Antimicrob Agents 2010;35(4):322–32.

[9] Kim H, Park H. Ginger extract inhibits biofilm formation by Pseudomonas aeruginosa PA14. PLoS One 2013;8(9):e76106.

[10] Bales PM, Renke EM, May SL, Shen Y, Nelson DC. Purification and characterization of biofilm-associated EPS exopolysaccharides from ESKAPE organisms and other pathogens. PLoS One 2013;8(6):e67950.

[11] Chew SC, Kundukad B, Seviour T, van der Maarel JRC, Yang L, Rice SA, Doyle P, Kjelleberg S. Dynamic remodeling of microbial biofilms by functionally distinct exopolysaccharides. mBio 2014;5(4).

[12] Sheppard DC, Howell PL. Biofilm exopolysaccharides of pathogenic fungi: lessons from bacteria. J Biol Chem 2016.

[13] Ophir T, Gutnick DL. A role for exopolysaccharides in the protection of microorganisms from desiccation. Appl Environ Microbiol 1994;60(2):740–5.

[14] Stoodley P, Sauer K, Davies DG, Costerton JW. Biofilms as complex differentiated communities. Annu Rev Microbiol 2002;56(1):187–209.

[15] Colvin KM, Gordon VD, Murakami K, Borlee BR, Wozniak DJ, Wong GCL, Parsek MR. The pel polysaccharide can serve a structural and protective role in the biofilm matrix of Pseudomonas aeruginosa. PLoS Pathog 2011;7(1):e1001264.

[16] Mishra M, Byrd MS, Sergeant S, Azad AK, Parsek MR, McPhail L, Schlesinger LS, Wozniak DJ. Pseudomonas aeruginosa Psl polysaccharide reduces neutrophil phagocytosis and the oxidative response by limiting complement-mediated opsonization. Cell Microbiol 2012;14(1):95–106.

[17] Costerton JW, Stewart PS, Greenberg EP. "Bacterial biofilms: a common cause of persistent infections.". Science 1999;284(5418):1318–22.

[18] Hansen SK, Rau MH, Johansen HK, Ciofu O, Jelsbak L, Yang L, Folkesson A, Jarmer HØ, Aanæs K, von Buchwald C, Høiby N, Molin S. Evolution and diversification of Pseudomonas aeruginosa in the paranasal sinuses of cystic fibrosis children have implications for chronic lung infection. ISME J 2011;6:31.

[19] Ryder C, Byrd M, Wozniak DJ. Role of polysaccharides in Pseudomonas aeruginosa biofilm development. Curr Opin Microbiol 2007;10(6):644–8.

[20] Ma LZ, Wang D, Liu Y, Zhang Z, Wozniak DJ. Regulation of biofilm exopolysaccharide biosynthesis and degradation in Pseudomonas aeruginosa. Annu Rev Microbiol 2022;76:413–33.

[21] Byrd MS, Sadovskaya I, Vinogradov E, Lu H, Sprinkle AB, Richardson SH, Ma L, Ralston B, Parsek MR, Anderson EM, Lam JS, Wozniak DJ. Genetic and biochemical analyses of the Pseudomonas aeruginosa Psl exopolysaccharide reveal overlapping roles for polysaccharide synthesis enzymes in Psl and LPS production. Mol Microbiol 2009;73(4):622–38.

[22] Billings N, Millan M, Caldara M, Rusconi R, Tarasova Y, Stocker R, Ribbeck K. The extracellular matrix Component Psl provides fast-acting antibiotic defense in Pseudomonas aeruginosa biofilms. PLoS Pathog 2013;9(8):e1003526.

[23] Billings N, Ramirez Millan M, Caldara M, Rusconi R, Tarasova Y, Stocker R, Ribbeck K. The extracellular matrix component psl provides fast-acting antibiotic defense in Pseudomonas aeruginosa biofilms. PLoS Pathog 2013;9(8):e1003526.

[24] Friedman L, Kolter R. Two genetic loci produce distinct carbohydrate-rich structural components of the Pseudomonas aeruginosa biofilm matrix. J Bacteriol 2004;186(14):4457–65.

[25] Ma L, Jackson KD, Landry RM, Parsek MR, Wozniak DJ. Analysis of Pseudomonas aeruginosa conditional psl variants reveals roles for the psl polysaccharide in adhesion and maintaining biofilm structure postattachment. J Bacteriol 2006;188(23):8213–21.

[26] Yu S, Su T, Wu H, Liu S, Wang D, Zhao T, Jin Z, Du W, Zhu M-J, Chua SL, Yang L, Zhu D, Gu L, Ma LZ. PslG, a self-produced glycosyl hydrolase, triggers biofilm disassembly by disrupting exopolysaccharide matrix. Cell Res 2015;25(12):1352–67.

[27] Zhang J, Wu H, Wang D, Wang L, Cui Y, Zhang C, Zhao K, Ma L. Intracellular glycosyl hydrolase PslG shapes bacterial cell fate, signaling, and the biofilm development of Pseudomonas aeruginosa. Elife 2022;11.

[28] Baker P, Hill PJ, Snarr BD, Alnabelseya N, Pestrak MJ, Lee MJ, Jennings LK, Tam J, Melnyk RA, Parsek MR, Sheppard DC, Wozniak DJ, Howell PL. Exopolysaccharide biosynthetic glycoside hydrolases can be utilized to disrupt and prevent Pseudomonas aeruginosa biofilms. Sci Adv 2016;2(5).

[29] Fleming D, Chahin L, Rumbaugh K. Glycoside hydrolases degrade polymicrobial bacterial biofilms in wounds. Antimicrob Agents Chemother 2017;61(2).

[30] Nilsson M, Chiang WC, Fazli M, Gjermansen M, Givskov M, Tolker-Nielsen T. Influence of putative exopolysaccharide genes on Pseudomonas putida KT2440 biofilm stability. Environ Microbiol 2011;13(5):1357–69.

[31] Wan Dagang WR, Bowen J, O'Keeffe J, Robbins PT, Zhang Z. Adhesion of Pseudomonas fluorescens biofilms to glass, stainless steel and cellulose. Biotechnol Lett 2016;38(5):787–92.

[32] Wang D, Xu A, Elmerich C, Ma LZ. Biofilm formation enables free-living nitrogen-fixing rhizobacteria to fix nitrogen under aerobic conditions. ISME J 2017;11(7):1602–13.

[33] Farias GA, Olmedilla A, Gallegos MT. Visualization and characterization of Pseudomonas syringae pv. tomato DC3000 pellicles. Microb Biotechnol 2019;12(4):688–702.

[34] Ye L, Matthijs S, Bodilis J, Hildebrand F, Raes J, Cornelis P. Analysis of the draft genome of Pseudomonas fluorescens ATCC17400 indicates a capacity to take up iron from a wide range of sources, including different exogenous pyoverdines. Biometals 2014;27(4):633–44.

[35] Vermeiren H, Willems A, Schoofs G, de Mot R, Keijers V, Hai W, Vanderleyden J. The rice inoculant strain Alcaligenes faecalis A15 is a nitrogen-fixing Pseudomonas stutzeri. Syst Appl Microbiol 1999;22(2):215–24.

[36] Monti MR, Smania AM, Fabro G, Alvarez ME, Argarana CE. Engineering Pseudomonas fluorescens for biodegradation of 2,4-dinitrotoluene. Appl Environ Microbiol 2005;71(12):8864–72.

[37] Xue Y, Qiu T, Sun Z, Liu F, Yu B. Mercury bioremediation by engineered Pseudomonas putida KT2440 with adaptationally optimized biosecurity circuit. Environ Microbiol 2022;24(7):3022–36.

[38] Xin XF, He SY. Pseudomonas syringae pv. tomato DC3000: a model pathogen for probing disease susceptibility and hormone signaling in plants. Annu Rev Phytopathol 2013;51:473–98.

[39] Jensen SE, Facycz IT, Campbell JN. Nutritional factors controlling exocellular protease production by Pseudomonas aeruginosa. J Bacteriol 1980;144:844–7.

[40] Franche C, Elmerich C. Physiological properties and plasmid content of several strains of Azospirillum brasilense and A. lipoferum. Ann Microbiol (Paris) 1981;132A:3–18.

[41] Yan X, Zhang Q, Zou J, He C, Tao J. Selection of optimized reference genes for qRT-PCR normalization in xanthomonas campestris pv. campestris cultured in different media. Curr Microbiol 2019;76(5):613–9.

[42] O'Toole GA, Kolter R. Initiation of biofilm formation in Pseudomonas fluorescens WCS365 proceeds via multiple, convergent signalling pathways: a genetic analysis. Mol Microbiol 1998;28(3):449–61.

[43] Hinsa SM, O'Toole GA. Biofilm formation by Pseudomonas fluorescens WCS365: a role for LapD. Microbiology 2006;152(Pt 5):1375–83.

[44] Yang J, Roy A, Zhang Y. Protein-ligand binding site recognition using complementary binding-specific substructure comparison and sequence profile alignment. Bioinformatics 2013;29:2588–95.

[45] Zheng L, Baumann U, Reymond J-L. An efficient one-step site-directed and site-saturation mutagenesis protocol. Nucleic Acids Res 2004;32(14). e115-e115.

[46] O'Toole GA. Microtiter dish biofilm formation assay. J Vis Exp 2011;47:2437.

[47] Heydorn A, Nielsen AT, Hentzer M, Sternberg C, Givskov M, Ersbøll BK, et al. Quantification of biofilm structures by the novel computer program COMSTAT. Microbiology (Reading) 2000;146(Pt 10):2395–407. https://doi.org/10.1099/00221287-146-10-2395.

[48] Costerton JW, Lewandowski Z, Caldwell DE, Korber DR, Lappin-Scott HM. " microbial biofilms.". Annu Rev Microbiol 1995;49:711–45.

[49] Attinger C, Wolcott R. Clinically addressing biofilm in chronic wounds. Adv Wound Care 2012;1(3):127–32.

[50] Rogers SA, Huigens RW, Cavanagh J, Melander C. Synergistic effects between conventional antibiotics and 2-aminoimidazole-derived antibiofilm agents. Antimicrob Agents Chemother 2010;54(5):2112–8.

[51] Izano EA, Wang H, Ragunath C, Ramasubbu N, Jb K. Detachment and killing of Aggregatibacter actinomycetemcomitans biofilms by dispersin B and SDS. J Dent Res 2007;86:618–22. https://doi.org/10.1177/154405910708600707.

[52] Tetz GV, Artemenko NK, Tetz VV. Effect of DNase and antibiotics on biofilm characteristics. Antimicrob Agents Chemother 2009;53(3):1204–9.

[53] Kalpana BJ, Aarthy S, Pandian SK. Antibiofilm activity of α-amylase from Bacillus subtilis S8-18 against biofilm forming human bacterial pathogens. Appl Biochem Biotechnol 2012;167(6):1778–94.

[54] Allen PZ, Whelan W. The mechanism of carbohydrase action.9. Hydrolysis of salep mannan by preparations of alpha-amylase. Biochem. J. Agric. Food Chem. 1963; 88:69–70.

[55] Wong-Madden ST, Landry D. Purification and characterization of novel glycosidases from the bacterial genus Xanthomonas. Glycobiology 1995;5:19–28.

[56] Algburi A, Comito N, Kashtanov D, Dicks LMT, Chikindas ML. Control of biofilm formation: antibiotics and beyond. Appl Environ Microbiol 2017;83(3).